Proceedings of the 2nd International Conference on Computing Innovation and Applied Physics
DOI: 10.54254/2753-8818/18/20230365

Optimization of the two-dimensional stator

Yulong Liang

Shenyang Aerospace University, No.37 Daoyi South Avenue, Daoyi District, Shenyang, Liaoning Province, China.

13591359072@163.com

Abstract. Gas turbine engine is mainly composed of compressor, inlet , tail nozzle, combustion chamber and turbine. The compressor pressurizes the air from the inlet into high-pressure air, which is used to mix and burn with fuel in the combustion chamber to form high-pressure gas. In this paper, numerical analysis of compressor stator performance and corresponding optimization were conducted using COMSOL Multiphysics 5.6. Firstly, an overview of compressor blade design is given. Then, the physical model and computational model are introduced and established by COMSOL. Afterwards, after the validation of the computational model, the numerical computations and results are generated and used to compare with NASA67 stator experimental data, with several key performance indicators including turning angle and loss coefficient. The polynomial expression is used to construct the blade shape/profile with different maximum thickness and its position, maximum bending and its position, trailing and leading edge angle and chord length are chosen as parameters for optimization. Then, I choose the maximum thickness and its position, maximum bending and its position, trailing and leading edge angle as the optimization parameter. Finally, we reach some conclusions of a better stator design possible for newer compressor requirements and further studies are recommended.

Keywords: optimization, stator, compressor.

1. Introduction

In 1971, the U.S. Air Force Aviation propulsion laboratory designed an axial-flow compressor rotor with a single-stage pressure ratio of up to 3.0 with a conventional scheme, but the experiment proved that all performance indicators were completely unqualified. In order to solve the problem, Wenner Strom proposed a technical scheme of large and small blade rotors in 1974 and a description was introduced in [1], but due to the limitation of computer technology at that time, there was a lack of effective technical analysis means, and the designed rotors still did not meet the standard. It was not until the early 1990s that the full three-dimensional numerical simulation technology was introduced into the compressor design and analysis that this technology made a breakthrough like [2]. The United States has restarted the research on aerodynamic technology of large and small blades. Many advanced designs of the blade of the compressor have been worked out recently and they may focus on difference areas such as low Reynolds number in [3].

However, for half a century, aviation gas turbine engines have been developing for high thrust weight ratio, high reliability, low fuel consumption, low cost and long working life. As one of the core components of aviation gas turbine engine, the boost ratio and efficiency of compressor will directly

© 2023 The Authors. This is an open access article distributed under the terms of the Creative Commons Attribution License 4.0 (https://creativecommons.org/licenses/by/4.0/).

DOI: 10.54254/2753-8818/18/20230365

affect the thrust weight ratio, thrust and fuel consumption of aviation gas turbine engine. The progress of its design technology will directly promote the improvement of the overall design level of aviation engine. The development requirements of aviation gas turbine engine for high-performance compressor are to ensure high efficiency and reduce compressor stages with sufficient stable operating margin. Single crystal superalloys have been developed to the third generation.

In the 1980s, people began to develop ceramic blade materials, and began to use anti-corrosion, heat insulation coating and other technologies on the blades. The GE90-115B engine produced by general motors of the United States has 22 turbofan blades with a single weight of 30-50 pounds and a total weight of 2000 pounds. The blade body is made of carbon fiber polymer materials and the blade edge is made of titanium alloy materials. It can provide the highest thrust to weight ratio. It is the largest aircraft jet engine blade at present. It is used for Boeing 777 aircraft and will be exhibited at the Museum of modern art in New York in September 2021. In [4], a geometry parameterization technique combined MISES and a single-objective genetic optimization algorithm with a suitable objective function. In [5], it combines an optimization with a geometry definition consisting of a small number of variables and was applied on all stator airfoil sections.

2. Basic setting of the model

2.1. Governing equations (turbulent model is k-ε model)

Continuity equation: $\frac{\partial \rho}{\partial t} + \nabla \cdot (\rho \vec{u}) = 0$

Navier-Stokes equation:

$$\rho \frac{D\vec{u}}{Dt} = \rho f - \nabla p + \mu^2 \nabla^2 \vec{u}$$

Specific equation of k-ε:

$$\rho(\vec{u} \cdot \nabla)k = \nabla \cdot [\left(\mu + \frac{\mu_T}{\sigma_k}\right) \nabla k] + P_k - \rho\varepsilon$$

$$\rho(\vec{u} \cdot \nabla)\varepsilon = \nabla \cdot \left[\left(\mu + \frac{\mu_T}{\sigma_\varepsilon}\right) \nabla \varepsilon\right] + C_{\varepsilon_1} \frac{\varepsilon}{k} P_k - C_{\varepsilon_2} \rho \frac{\varepsilon^2}{k} \quad , \quad \varepsilon = ek$$

2.2. Boundary conditions

In this study, for the fluid flow, no flow through and no slip boundary conditions are applied at the wall of the airfoil profile. For the inlet, we define a normal velocity and for the outlet we define constant pressure. For the upper and lower boundary of computational area, we use periodic boundary condition to simulate the annual distribution of stator blades. No flow through (v_norm = 0), no slip (v_tan = 0), periodic boundary, inlet, outlet.

2.3. Dimension and key performance parameters

In the stator blade, we generally pay attention to the total pressure loss and the turning angle of the air flow, because the main role of the stator blade is to change the direction of the air flow. Meanwhile, the pressure increase generally occurs in the moving blade, and the pressure loss is considered in the whole compressor stage.

Total-loss coefficient (the representation of much total pressure has lost during the flow through the stator): $\omega = \frac{p_{in}^* - p_{out}^*}{p_{in}^* - p_{in}}$

In Reynolds number, $Re = \frac{\rho v d}{\mu}$, d represents the chord of the stator and μ represents the air viscosity coefficient. Re is between 39000 to 41000.

Flow turning angle (the change of the direction of the air flow) : $\Delta\beta = \beta_{in} - \beta_{out}$

DOI: 10.54254/2753-8818/18/20230365

Attack angle (the relative angle of the coming air flow): $i=\beta_{in}-\beta_{out}$

Pressure coefficient (the measure of pressure): $C_p=\frac{p-p_\infty}{\frac{1}{2}\rho_\infty v_\infty^2}$

Our optimization goal is to consider the lost coefficient and the turning angle at the same time and the formula is: $0.65*\omega+0.35*\Delta\beta$.

2.4. Computational model(numerical model)

First, separate the data of NASA67 into camber equation(yf(x))and thickness equation(yc(x)), then fitting with quintic functions. The upper line of the stator is yf(x)+yc(x) and the down one is yf(x)-yc(x).

Second, use leading edge angle, trailing edge angle, maximum camber, position of the maximum camber, chord length and difference between the height of the first and the last point to replace the coefficients of the quintic function of the chamber. Using maximum thickness and its position to replace the coefficients of the quintic of the function of the thickness.

2.5. Mesh

It is produced by COMSOL5.6 which provides advanced geometry acquisition, mesh optimization tools and mesh generation to fulfill the requirement for integrated mesh generation for sophisticated analyses. However, its density varies a lot at the place of great curvature. So defining a more effective way by constraining meshes in some predefined squares is essential. Through this way, the amount of meshes will not vary a lot and they will be evenly distributed. Boundary layers have 10 layers, the boundary layer stretching factor is 1.1 and the thickness factor is 1.2.

Figure 1 is the mesh of the stator.

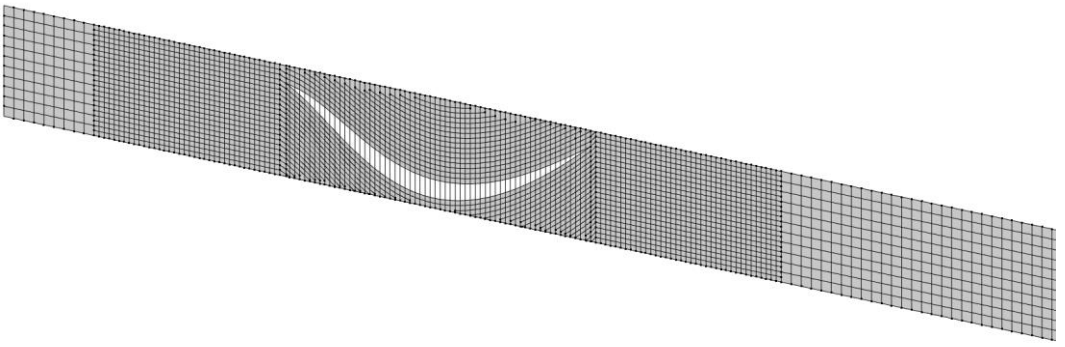

Figure 1. Mesh of the stator.

3. Examination of model

3.1. Computational configurations

The iteration of CFD solver went below the maximum residual within 118 steps. The efficiency monitor, velocity and pressure monitor and turbulence monitor all worked normally and results were reasonable.

DOI: 10.54254/2753-8818/18/20230365

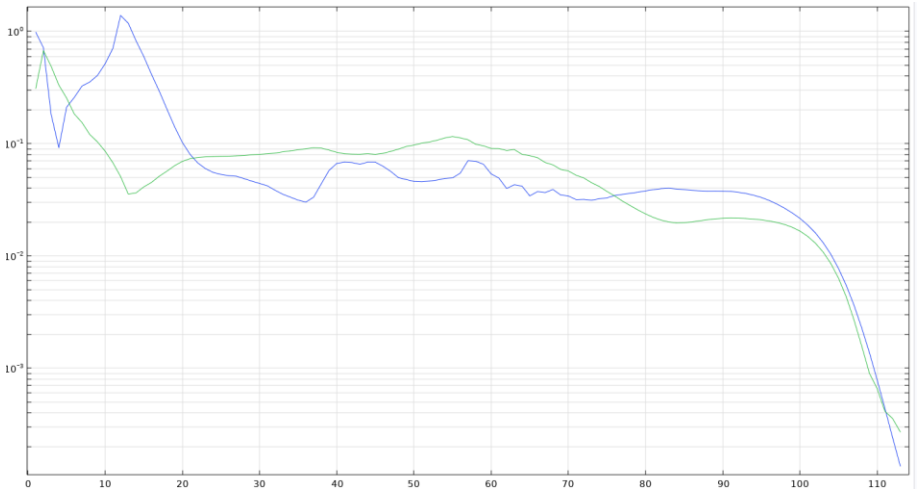

Figure 2. Monitor, mass and momentum monitor and turbulence monitor.

The efficiency monitor, mass and momentum monitor and turbulence monitor all worked normally and results were reasonable. During the optimization, Nelder-Mead calculating method is used.

3.2. Mesh sensitivity study

In order to validate the computational results, a mesh sensitivity study was conducted first by choosing the average velocity of the entrance as characteristic parameter and the results are shown in Table below. As can be seen from the table, case 1,2 compared with case 3, still have a relative difference of 0.28%, while for case 3 and 4, the difference is relatively small enough. Therefore, we consider mesh for case 3 is fine enough so that the computed results will not be affected by the meshes.

Table 1. Different cases of the model.

case number	number of mesh elements	characteristic parameter value	relative difference	Line color
1	97125	0.916102	0.291257%	yellow
2	100,183	0.916115	0.289842%	red
3	133682	0.919445	0.072597%	green
4	164,393	0.918778	0	blue

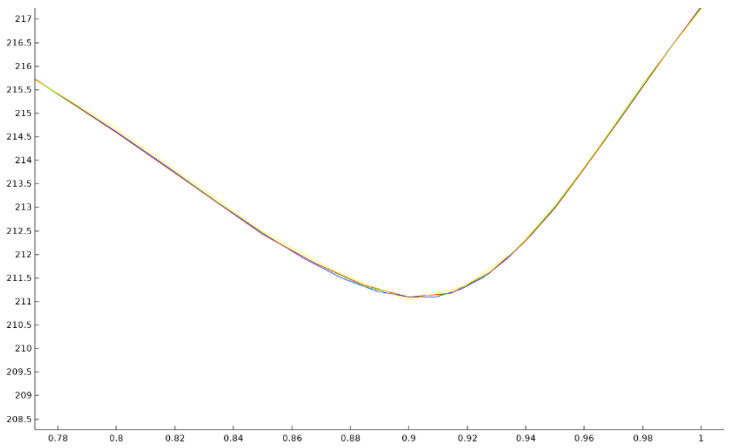

Figure 3. The average velocity in front of the entrance of the stator.

DOI: 10.54254/2753-8818/18/20230365

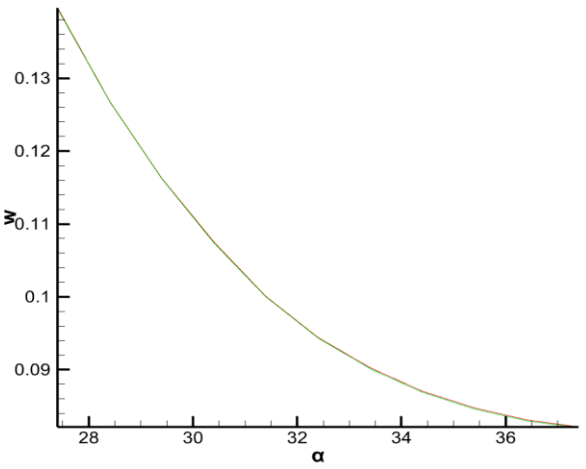

Figure 4. The comparation of ω of my own simulation of NASA67 and the standard one.

Therefore, conclusion can be drawn from the results of Figure 3 and Figure 4 that 97125 nodes is enough for simulation to be conducted independent of mesh density. The designed stator will use the same meshing method and calculation conditions to ensure that the results change only because of profile.

4. Results and analyses

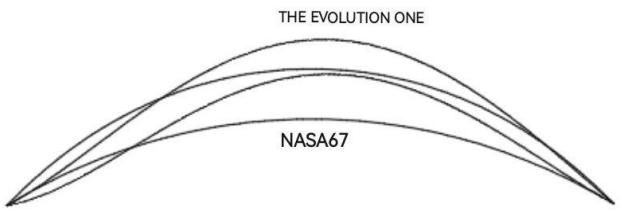

Figure 5. The comparison of the evolution stator and NASA67.

The optimized profile has more maximum bending and it obviously represents a greater turning angle of the airflow.

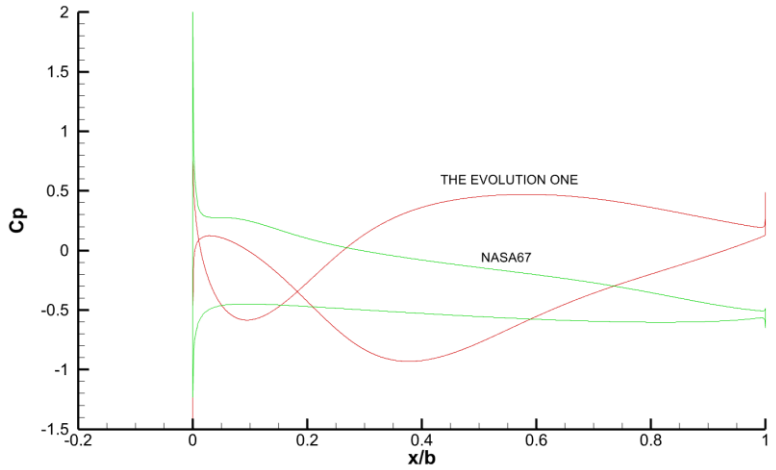

Figure 6. The comparison of c_p of the evolution stator and NASA67.

Figure 6 shows the distribution of one of the key performance parameters of the profile along chord length, which is c_p. As can be seen from the figure, the pressure is mostly concentrated at 13% and 52% of chord length. Also, it doesn't have a sharp decrease or increase throughout the whole chord compared to NASA67 profile, so its torsional moment is less.

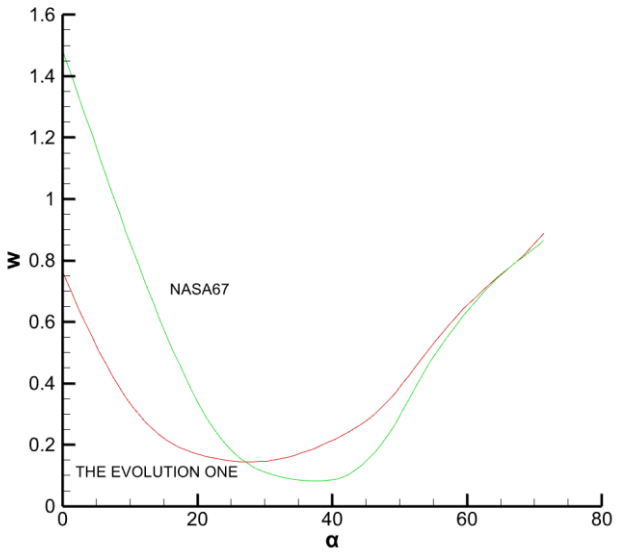

Figure 7. The comparison of loss coefficient of the evolution stator and NASA67.

Figure 7 illustrates the loss coefficient ω related to the attack angle for NASA67 and also the optimized profile. As can be observed, the loss coefficient is lower when the angle of attack is in the range of 0~26 degrees. The typical working attack angle for this kind of stator blade is usually0~26 degrees, and therefore we decreased the loss in majority of the working range. It is noticeable that the optimized profile has a wider low-loss range than NASA67, although the lowest loss coefficient is slightly higher.

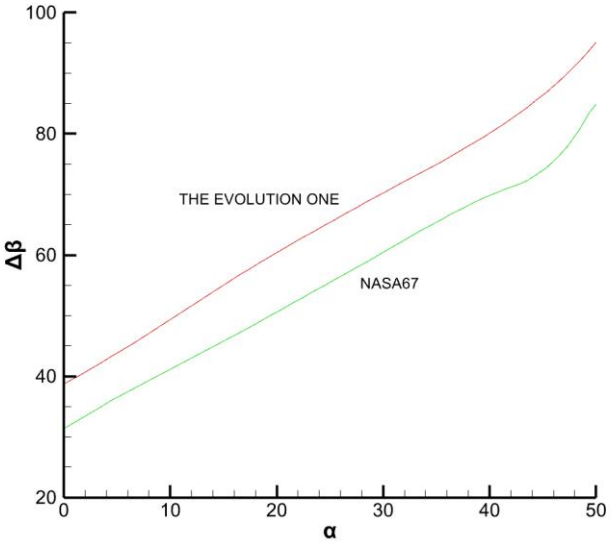

Figure 8. The comparison of flow turning angle of the evolution stator and NASA67.

Figure 8 shows the flow turning angle $\Delta\beta$ related to attack angle for NASA67 and optimized profile. From the figure, we can see that at certain attack angle, the optimized profile always gives a greater turning angle than NASA67, indicating that the possibility for the profile to reach certain design limits without stalling.

5. Summaries of discoveries

In a nutshell, a profile optimization method for the stator of a high Reynolds and high subsonic number axial compressor stage has been shown. This method combines an optimization with a geometry definition consisting of a few variables and was applied on the stator sections. Through the optimization, the pressure distribution is more even and the turning angle has increased 9 degrees. Also, the lost coefficient has decreased 70 percent to 50 percent while the attack angle is between 0 and 20 degrees.

Future research should concentrate on the optimization weighting factors in terms of the design method. What's more, in the on-going research project, the application to aero engine stators should be pursued to achieve a favorable effect, considering the actual working condition of the blade.

References

[1] Schlichting, H., and Truckenbrodt, E. (1979) Aerodynamics of the Airplane (Translated by H. J. Ramm). McGraw-Hill International Book Company.
[2] Kulfan, B. M., and Bussoletti, J. E. (2006). Fundamental parametric geometry representations for aircraft component shapes. AIAA Paper 2006-6948, 1-45.
[3] Schreiber, H. A., Steinert, W., Sonoda, T., and Arima, T. (2004). Advanced high-turning compressor airfoils for low Reynolds number condition - part II: Experimental and numerical analysis. J. Turbomachinery, 126 (4), 482-492. doi:10.1115/1.1737780
[4] Giesecke, D., Stark, U., Harms García, R., and Friedrichs, J. (2017). Design and Optimization of Compressor Airfoils by Using Class Function / Shape Function
[5] Methodology. 17th International Symposium on Transport Phenomena and Dynamics of Rotating Machinery (ISROMAC).
[6] Daniel Giesecke, Marcel Bullert, Jens Friedrichs TU Braunschweig (2018). Optimization of high subsonic, high Reynolds number axial compressor airflow sections for increasing operating range. GPPS-2018-47